Cumhuriyet Sci. J., 46(1) (2025) 62-72
DOI: https://doi.org/10.17776/csj.1487341

Cumhuriyet Science Journal

| csj.cumhuriyet.edu.tr | Founded: 2002 ISSN: 2587-2680 e-ISSN: 2587-246X Publisher: Sivas Cumhuriyet University

A New Candidate for the Treatment of Alzheimer's Disease; Synthesis, Characterization, Investigation of Drug Properties with *In Silico* Methods

Ömer Dilek [1,a,*], Tolga Acar Yeşil [2,b], Tahir Tilki [3,c]

[1]*Central Research Laboratory Application and Research Center, Isparta University of Applied Sciences, Isparta, Türkiye*

[2]*Department of Property Protection and Security, Türkeli Vocational School, Sinop University, Sinop, Türkiye*

[3]*Department of Chemistry, Faculty of Engineering and Natural Sciences, Süleyman Demirel University, Isparta, Türkiye*

**Corresponding author*

Research Article

History
Received: 21/05/2024
Accepted: 30/01/2025

ABSTRACT

Brain disorder-caused mortality has emerged as the second of all diseases worldwide in the 21st century. Alzheimer's Disease (AD) is the most common disease that takes place among brain disorders according to statistics. Therefore, in this study, potential new drug candidate for AD (2-**a**mino-N'-**b**enzylidene-4-(**t**rifluoromethyl)benzo**h**ydrazide, ABTH) was synthesized, starting from -CF_3 and -NO_2 containing carboxylic acid. The structure of ABTH was elucidated using ^1H, ^{13}C-APT NMR, FTIR, and Mass analyses. ADMEt properties were calculated and from the ADMEt results, it was observed that the ABTH crossed the Blood-Brain Barrier (BBB), the most important property in evaluating new drug candidate in brain disorders. Molecular Docking studies were conducted using proteins related AD. According to docking studies, 2OI0-ABTH was the highest docking score with the -8.9 kcal/mol. Standard drugs (Donepezil, Galantamine, Rivastigmine) used in AD treatment were also docked with the AD proteins to do meaningful comparison. The molecular docking results showed that the ABTH has higher docking score than standards. Since 2OI0-ABTH complex had the best docking score, it was chosen for the MD simulation studies. From the obtained results, It can be suggested that ABTH promising drug candidate for AD after further investigations were done.

Keywords: Alzheimer's disease, Fluorine compounds, Hydrazone, ADMEt, Molecular docking.

[a] omerdilek@isparta.edu.tr https://orcid.org/0000-0003-1409-782X
[b] tyesil@sinop.edu.tr https://orcid.org/0000-0001-5983-8447
[c] tahirtilki@sdu.edu.tr https://orcid.org/0000-0002-1040-2375

Introduction

As the world's population ages in the 21st century, brain diseases, which globally rank as the second most common cause of mortality, such as brain tumors, stroke, neurodegenerative diseases, and other catastrophic illnesses, have grown to pose a serious threat to human life and health [1]. A variety of techniques are used in the current treatment of brain diseases, such as radiation therapy, chemotherapy, and surgery, which are used to treat brain tumors [2]. Based on their causes, symptoms, and effects on the brain, brain disorders can be classified into various categories and impact numerous aspects of brain function. Some common types of brain diseases are dementia, brain cancer, epilepsy, mental disorders, stroke and transient ischemic attack, Parkinson's, and AD.

AD is a neurological illness that worsens over time and mostly impacts behavior, thinking, and memory. It is the most typical cause of dementia, a syndrome marked by a significant enough reduction in cognitive function to cause problems in day-to-day functioning [3]. With a global prevalence of 24 to 34 million cases, AD is the most frequent type of dementia [4]. A variety of proteins, including tau protein, β-amyloid (Aβ), and amyloid precursor protein (APP), are important in the progression and course of AD [5].

Fluorine is known to have a major impact on chemical reactivity, physicochemical behavior, and biological activity due to its size, electronegativity, lipophilicity, and electrostatic interactions [6]. Fluorine's beneficial effects on pharmacological properties have led to a growing interest in fluorinated group (such as F, CF_3, OCF_3, CHF_2, etc.) substances [7].

Hydrazones can be combined with other functional groups to create molecules with distinct chemical and physical properties [8]. Their biological and pharmacological properties make them valuable for the synthesis of heterocyclic compounds and development of new drugs [9]. The biological features of these molecules are noteworthy and include antibacterial, antiviral, analgesic, antidepressant, anticancer, and anti-neuroinflammatory effects [10]. Potential therapies for AD are now being researched, including pharmacologically active hydrazone derivatives with anti-neuroinflammatory potential [11].

The process of developing a new drug can take up to 10-15 years on average, and it can cost up to $255.8 million to bring a drug to market [12]. Furthermore, only 13% of clinical studies reported in literature for new pharmacological drugs are successful [13]. As a result, in the last few decades, the application of in silico methods

for drug discovery like computer-aided drug design (CADD) has increased significantly [14]. Applications of CADD typically assist in experimental research decision-making by monitoring the major stages of drug development, such as target validation, hit discovery, lead generation, and optimization [15]. CADD mainly deals with drug design based on ligand structure and drug design based on receptors. When developing new drugs, one of the most crucial ADME and Toxicity properties take into account is the BBB permeability of the compounds. The BBB, is a complex biological structure that separates the brain from the systemic blood circulation and is responsible for preserving the homeostasis of the central nervous system (CNS) [16]. The ability of compounds to penetrate the BBB determines how possible drugs are distributed between the blood and the brain. Lipophilic drugs can easily penetrate the BBB through passive diffusion. In contrast, polar molecules are typically unable to pass through the BBB, however occasionally an active transport process can help them [17]. Effective permeability of the BBB is a vital requirement for the development of new drugs intended to treat brain diseases. Molecular docking has increased in significance as an *in silico* drug discovery approach. By modeling the atomic-level interaction between a small molecule and a protein using the molecular docking approach, we can clarify basic biochemical processes and characterize the behavior of small molecules at target protein binding sites [18]. In recent years, MD simulations have become increasingly important in the drug discovery process. MD simulations, which depend on a general model of the physics controlling interatomic interactions, forecast the position of each atom in a protein or other molecular system across time [19].

Because of specified reasons above the ABTH was synthesized. Its structure was verified by using NMR, FTIR, and Mass spectroscopic techniques. *In silico* ADMEt properties were calculated utilizing web servers. Protein-ligand interactions were investigated via Molecular Docking and MD Simulation studies. In molecular docking studies target proteins (PDB ID: 1AAP for amyloid precursor protein (APP); 1O86 for Angiotensin converting enzyme (ACE); 4DJU for β-site APP cleaving enzyme 1 (BACE1); 1Q5K for Glycogen synthase kinase-3 (GSK-3); 2OI0 for TNF-a converting enzyme (TACE)) related with AD were studied. The protein-ligand couple (2OI0-ABTH), which has the best docking score, was used in the MD simulation studies.

Material and Method

General Information

All chemicals used for synthesis and purification were purchased from Aldrich, Merck, and Isolab companies. All reaction conversions were followed by Thin Layer Chromatography (TLC: SIL G/UV254 from MN GmbH & Co). UV light (254 nm) was used for the visualization of spots. Melting points of synthesized compounds were measured in an open glass capillary tube using the Stuart SMP 30. NMR spectra were recorded by using an Agilent 400 MHz spectrometer and DMSO-d_6 as solvent. Chemical shifts were specified as ppm. Chemical shifts of remaining solvent were adjusted to 2.5 ppm for ^{1}H-NMR, 39.52 ppm for ^{13}C-NMR. A Shimadzu IR Prestige-21 device was used to record FTIR analysis with KBR pellet technique. For mass analyses, the Waters Radian Asap Direct Mass Detector was used. The analytical methods included full scan acquisition mode, ASAP+/ASAP ionization mode, gas (N_2), mass range 100-1200 m/z, cone voltage 10 V, isothermal heater temperature of 600 °C, corona current 3 µA, and capillary dip sampling technique.

Synthesis and Characterization Studies

Synthesis of 2-amino-4-(trifluoromethyl)benzohydrazide (3)

A 100 mL round bottomed two necked flask that was equipped with a magnetic stirring bar and reflux condenser, was charged with 2-nitro-4-(trifluoromethyl)benzoic acid (1, 42.6 mmol; 10.0 g), 6 mL of H_2SO_4 and 100 mL methanol. The flask was heated to reflux via an oil bath for 48 hours. The conversion was also checked by TLC in 6 hours periods. After 48 hours, it was observed that the conversion was completed. The mixture was poured into the cold water and pH was adjusted to 7 with saturated aqueous $NaHCO_3$ solution. Organic components were extracted with three times 100 mL EtOAc. The combined organic extracts were washed with water and brine. So, 10.2 g of the methyl 2-nitro-4-(trifluoromethyl)benzoate(2) was obtained as single product according to TLC in 96% yield. The crude product was converted to its aminohydrazide derivative by using hydrazine hydrate. The 100 mL round bottomed one necked flask containing 10.2 g of the methyl 2-nitro-4-(trifluoromethyl)benzoate and magnetic stirring bar, was charged with 50 mL of hydrazine hydrate, and refluxed for 3 hours. After 3 hours, it was observed that the starting material was converted into the hydrazide derivative. After 3 hours, excess hydrazine hydrate was removed under reduced pressure. The mixture was cooled to room temperature and 50 mL of cold water was added into the flask. The precipitate was filtered and dried. The dried crude product was crystallized with $CHCl_3$/Hexane mixture. 5.82 g of the title compound 2-amino-4-(trifluoromethyl)benzohydrazide (3) was obtained as white solid in 65% yield. Compound 3; Melting Point: 170–172 °C. MS = *m/z*: $[M+H]^+$ Calcd for $C_8H_9F_3N_3O$, 220.18; Found: 220.17.

Synthesis of ABTH

2-amino-4-(trifluoromethyl)benzohydrazide (1 mmol, 219 mg), benzaldehyde (1.1 mmol; 117 mg), catalytic amount AcOH (2-3 drop) and 20 mL absolute ethanol were added into the 100 mL two necked flask that was equipped with magnetic stirring bar and reflux condenser. The mixture was refluxed for 3 hours. The conversion was also followed by TLC. After 3 hours, it was observed that starting material was consumed. The ethanol was removed under reduced pressure. The crude product was

purified by column chromatography using EtOAC/hexane (v/v: 2/1) as eluent. 225 mg of the title compound (ABTH) was obtained in 73% yield. Melting Point: 206–208 °C. FTIR(KBr): $\tilde{\nu}_{max}$ (cm^{-1}) = 3521 (w), 3462 (w), 3394 (w), 3348 (w), 3223 (br), 3050 (w), 3029 (w), 1647 (s), 1593 (s), 1546 (s), 1437 (s), 1353 (s), 1331 (s), 1250 (s), 1166 (s), 1131 (s). ^{1}H-NMR (400 MHz, DMSO-d_6): δ 11.80 (s, 1H), 8.40 (s, 1H), 7.72 (s, 3H), 7.45 (m, 3H), 7.11 (d, J = 1.2 Hz, 1H), 6.86 (dd, J = 8.2, 1.4 Hz, 1H), 6.68 (s, 2H). ^{13}C{^{1}H}-NMR (APT, 101 MHz, DMSO-d_6):δ 164.20 (C=O), 149.92 (C), 147.75 (CH), 134.28 (C), [132.51, 132.20, 131.90, 131.59, (C, $J^2_{C\text{-}F}$ = 30.90 Hz)], 130.06 (CH), [129.59, 129.56, (CH, $J^4_{C\text{-}F}$ = 3.2 Hz)], 128.83 (CH), [128.02, 125.30, 122.59, 119.88, (C, $J^1_{C\text{-}F}$ = 272.60 Hz)], 127.05 (CH), 116.68 (C), [112.39, 112.36, (CH, $J^3_{C\text{-}F}$ = 3.77 Hz)], [110.27, 110.23, 110.20, 110.16, (CH, $J^3_{C\text{-}F}$ = 3.59 Hz)]. MS = m/z: $[M+H]^+$ Calcd for $C_{15}H_{13}F_3N_3O$, 308.10; Found: 308.18.

In silico Studies

ADMEt studies

Parameters, such as physicochemical properties, lipophilicity, water solubility, pharmacokinetic and druglikeness properties of the synthesized compound, which play an important role in determining the ADME parameters, were determined by using the SwissADME web server [20]. ProTox-II web server was used to calculate toxicity properties such as LD_{50} and toxicity class [21].

Molecular docking studies

Energy minimization of ABTH and standard drugs were performed by using Avagadro software and UFF parameters before the molecular docking studies [22]. AutodockVina 1.1.2 software was used for Molecular docking studies [23]. UCSF Chimera 1.17.3 for 3D [24] and BIOVIA Discovery Studio Visualizer [25] for 2D were used for all imaging processes. Target proteins specified with PDB ID in Table 1 were used for the molecular docking studies. Selected proteins were downloaded from PDB Bank as .pdb file [26]. All heteroatoms, waters, and non-standard residues were removed from the protein by using UCSF Chimera 1.17.3 software. Dockprep module of UCSF Chimera 1.17.3 was used to add Gasteiger charges. Modeller program was used to homologize selected proteins [27]. The 3D binding coordinates (x,y,z) of selected proteins were calculated utilizing DeepSite web server [28]. A grid box surrounding proteins was used during molecular docking studies.

Table 1. Target Proteins with the PDB ID and 3D binding coordinates

Target Protein	PDB ID	3D Binding Coordinates (x, y, z)
APP	1AAP	10.7; 18.2; 34.7
ACE	1O86	39.0; 39.2; 54.8
BACE1	4DJU	21.2; 32.5; 57.7
GSK-3	1Q5K	8.0; 34.8; 14.4
TACE	2OI0	45.2; 26.8; 1.0

MD simulation studies

Playmolecule web server was utilized for the MD simulation studies [29]. Initially, Force Field (FF) parameterization of ligand was performed by using parameterize module [30]. Then, all selected proteins were prepared for MD simulation with ProteinPrepare module [29]. For the preparing system to MD simulation, the SystemBuilder application based on Playmolecule was used. While the system was being prepared the salt concentration of NaCl was adjusted to 0.15 M. By using AMBER Force Field at 300 K and pH:7.4, the system was prepared for MD simulation. Finally, with the created system in the SystemBuilder of the MD simulation was started by using SimpleRunmodule [31]. MD Simulation was conducted during 12 ns.

Results and Discussion

Synthesis and Characterization

Scope of synthesis studies, the carboxylic acid derivative (1) was converted to its methylester (2) by using methanol and H_2SO_4. Then, we tried to convert methyl ester to its hydrazide derivative. According to mass analyses (Figure 1) result of obtained product, we observed that not only ester group was converted to hydrazide but also the reduction of nitro group to amine. The aminobenzohydrazide compound 3 was reacted with benzaldehyde (4) in absolute ethanol to give corresponding ABTH in 73% yield. Presence of amine group in the ABTH has also verified with NMR that the broad peak has two protons according to integration in the 6.68 ppm. The synthetic pathway was given in Figure 1. The structure of compound 3 was verified with only mass (Figure 2) and melting point analyses because of the compound commercial available while ABTH was verified with melting point, NMR, Mass, and FTIR analyses. While molecular weight of compound 3 has been theoretically calculated as 219.17 g/mol, it was experimentally observed as 220.17 g/mol in mass analyses in positive mode. The ABTH has eight aromatic region protons, two amine protons, one imine proton, and one hydrazide NH proton. When the ^{1}H-NMR spectrum of ABTH was examined (Figure 3); ^{1}H-NMR result showed that among 6.5-8.5 ppm contain total of eleven protons including aromatic region, amine, and imine protons, and hydrazide proton in the 11.80 ppm. When the ^{13}C-APT NMR spectrum was examined (Figure 4); number of aromatic CH and C carbon atoms was suitable for the suggested structure. Carbon atom of carbonyl group (C=O) was observed in 164.20 ppm. Carbon atom of CF_3 group was observed as a quartet signal among 128.02-119.88 with the 272.60 Hz coupling constant. The mass analysis also confirmed the suggested ABTH structure. While the calculated molecular weight of suggested structure was 307.28, It was observed in experimental mass spectra in the positive ionization mode as 308.18 (Figure 5). FTIR analysis of ABTH was also recorded by using KBr pellet technique. When the FTIR spectrum of ABTH was examined, the peaks seen among 3521-3223 cm^{-1} were related with -NH stretching, 3050 and 3029 cm^{-1} aromatic C-H stretching, 1647 cm^{-1} C=O stretching, 1593 C=N, 1546 N-N stretching (Figure 6). The specified peaks were also verified the structure.

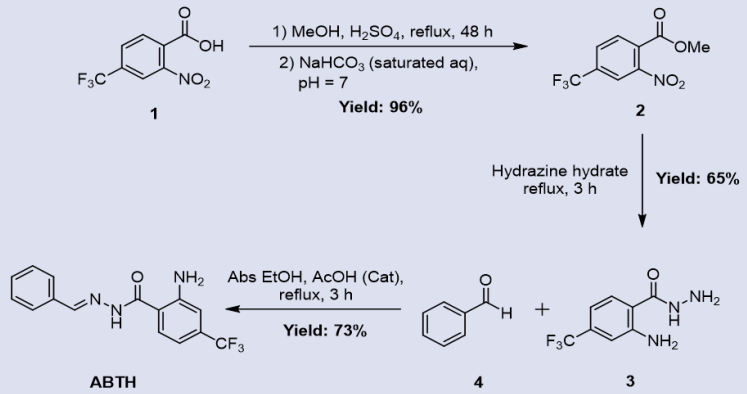

Figure 1. Reaction scheme for synthesis of ABTH

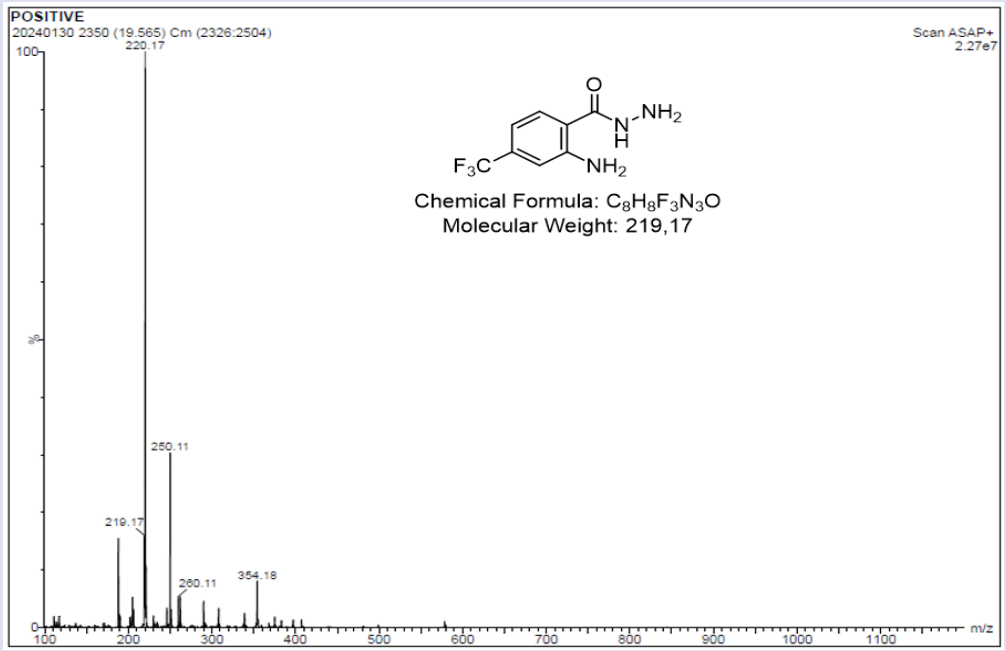

Figure 2. Mass Spectrum of compound 3

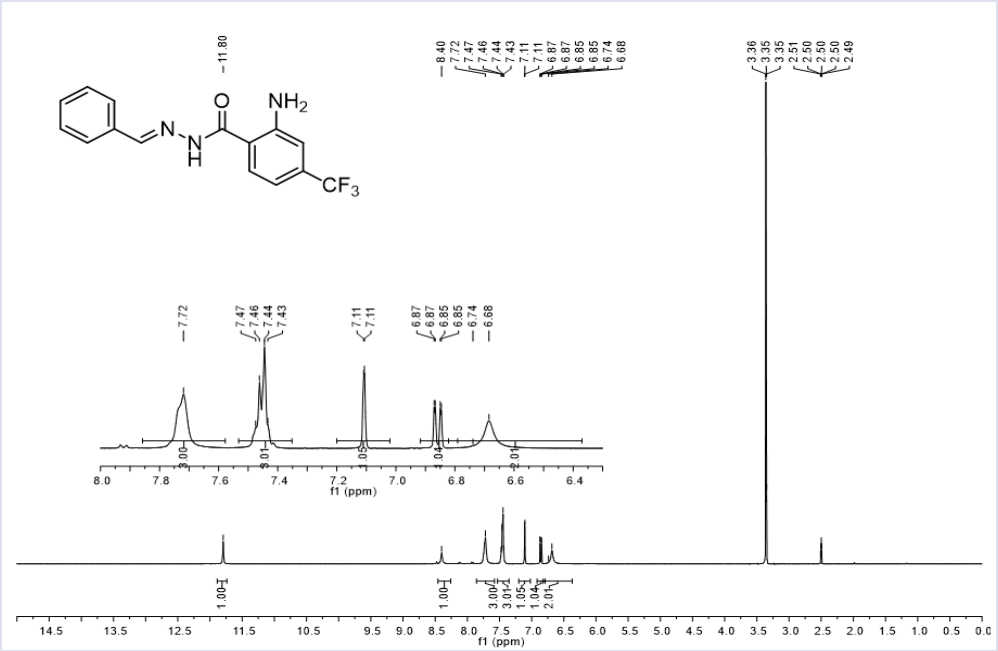

Figure 3. ^{1}H-NMR Spectrum of ABTH

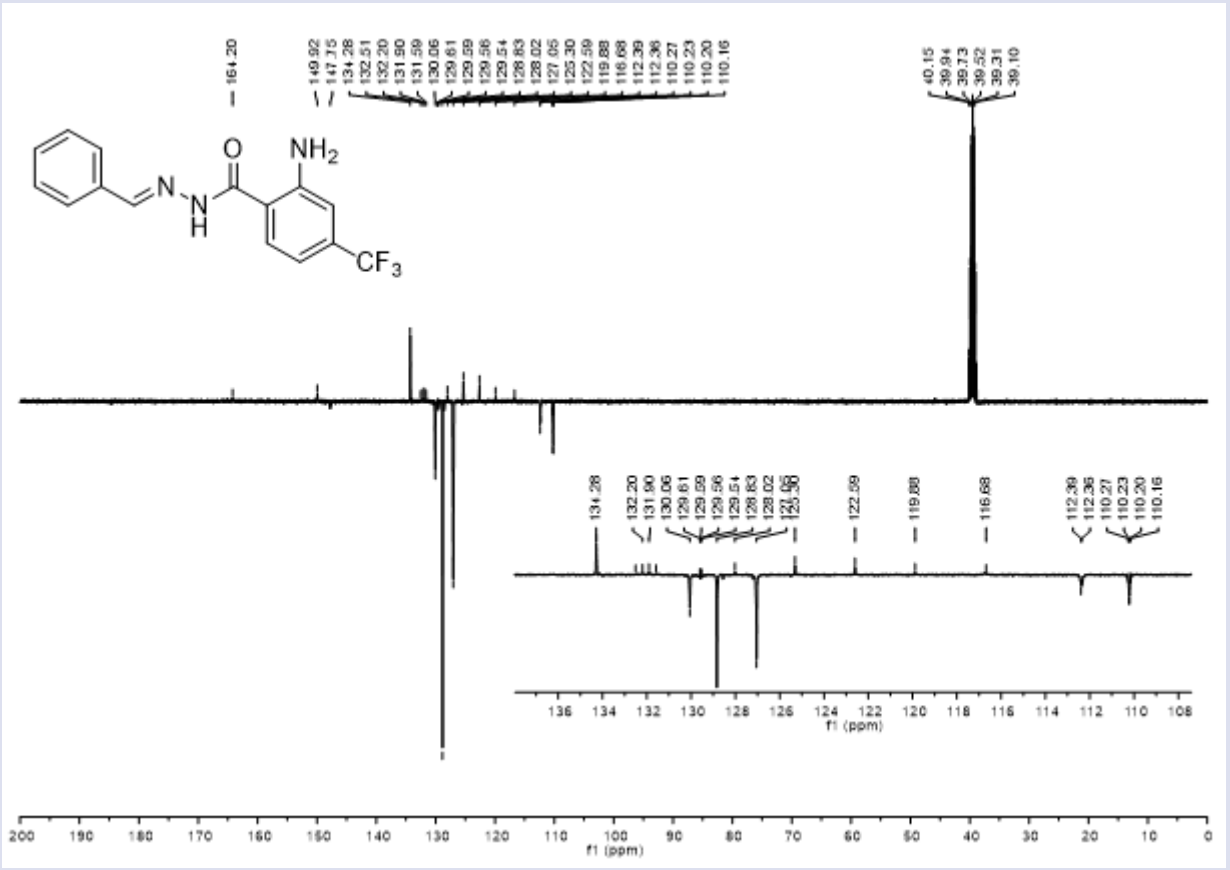

Figure 4. ^{13}C-NMR Spectrum of ABTH

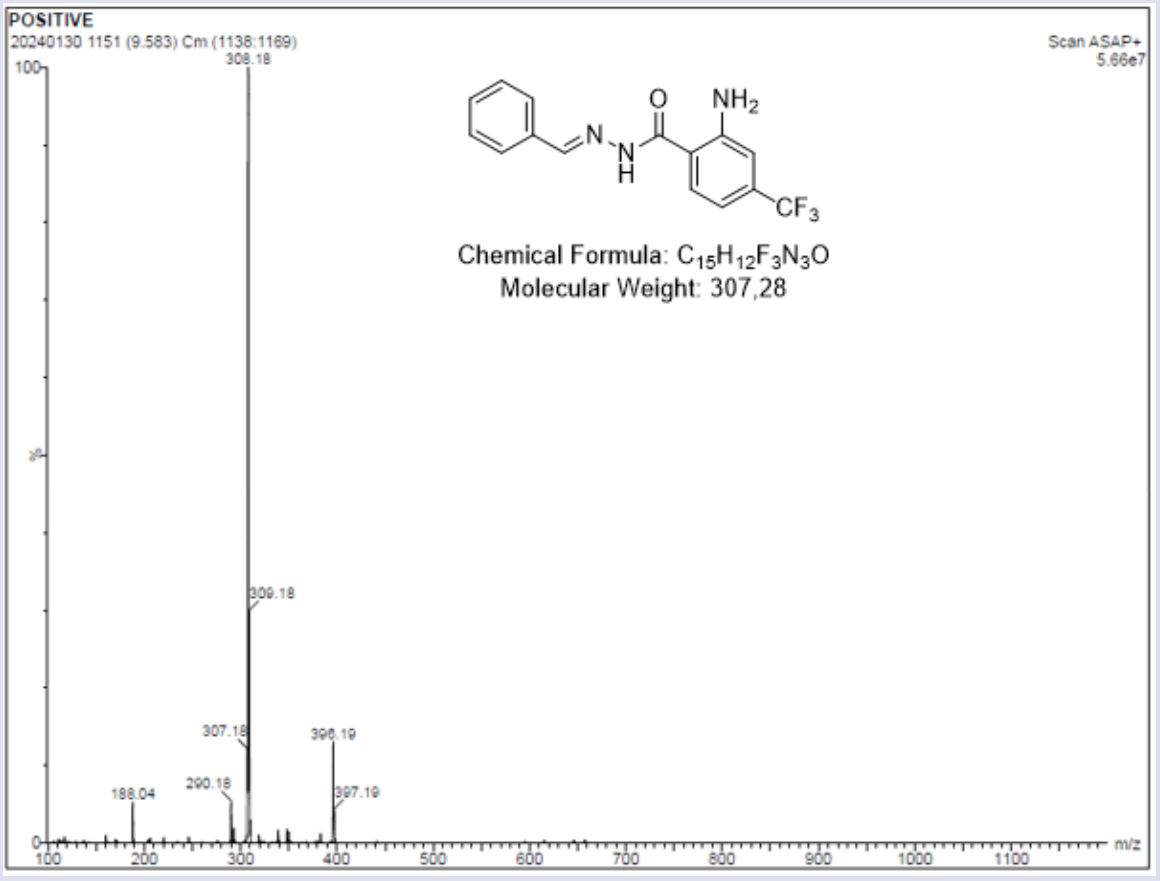

Figure 5. Mass Spectrum of ABTH

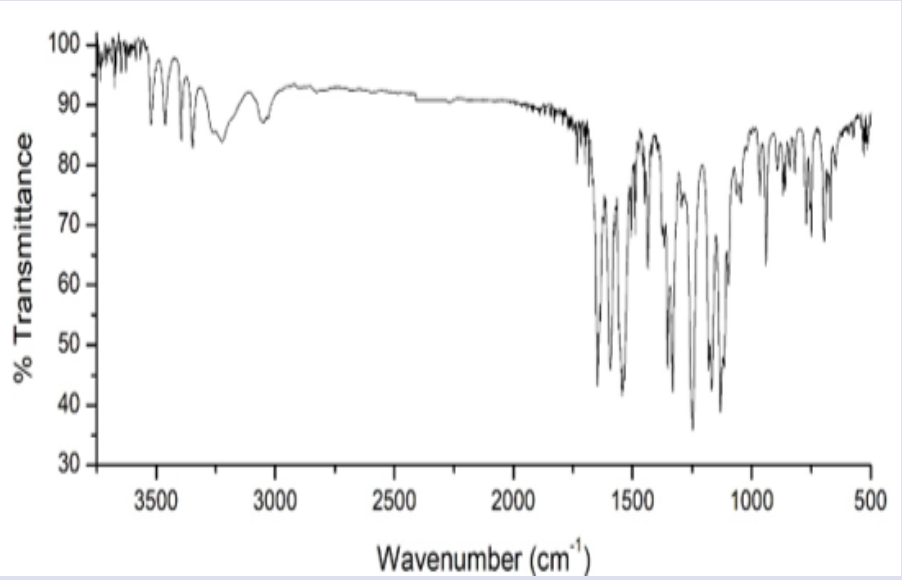

Figure 6. FTIR Spectrum of ABTH

In Silico Studies

ADMEt studies

The identification of ADMEt properties of new drug candidates are critical step in the development of any pharmaceutical compounds. Due to several reasons, including their improper pharmacokinetics and drug-likeness, most candidate compounds are eliminated. ADMEt properties of ABTH were depicted in Table 2.

Lipinski's rule of five is important for drug discovery. According to Lipinski's Rules, The drug candidate's molecular weight should be between 150 and 500 g/mol, MLOGP value < 4.15, The number of hydrogen bond acceptor (HBA) atoms < 10, and Number of hydrogen bond donor (HBD) atoms < 5. When ABTH was investigated for all criteria, it was observed that molecular weight of synthesized compound has 307.27 g/mol, MLOGP value has 3.17, HBA atoms have 5, HBD atoms have 2. According to results obtained from calculations, the ABTH compound has been suitable in terms of Lipinski's rule of five. The substance's Topological Polar Surface Area (TPSA) value, which should be less than 140 $Å^2$, is also significant since it determines how well compounds pass through cell membranes [32]. When the TPSA value of ABTH was examined in Table 2, It was lower than 140 $Å^2$ (67.48 $Å^2$). The dispersion of compounds at specified rates between lipids and water is known as lipophilicity. Drug molecules must pass through a number of biological membranes, including as the skin, the gut, and the blood-brain barrier, in order to reach their target areas. Consensus lipophilicity ($CLogP_{o/w}$) value of ABTH was determined to be 3.28.

Water solubility is a crucial property of drug candidates that influences their absorption, distribution, metabolism, and excretion (ADME). Highly soluble drugs dissolve readily in biological fluids, enhancing oral bioavailability and systemic absorption. However, excessively soluble drugs may be rapidly excreted, reducing their efficacy. Conversely, poorly water-soluble drugs often exhibit limited bioavailability and uneven tissue distribution, necessitating advanced formulation strategies to enhance solubility and absorption. Achieving an optimal balance of water solubility is essential for designing effective and pharmacokinetically favorable drug candidates [33]. When the calculated water solubility value was examined, it was -4.08 (ESOL) corresponding to moderately soluble.

In addition to their pharmacokinetic properties, cytochrome P450 enzyme systems are vital for the metabolism of medications that are ingested. Table 2 analysis revealed that CYP1A2 is likely to inhibit ABTH, whereas CYP2C9, CYP3A4, CYP2C19, and CYP2D6 are not likely to do so. Druglikeness skills were examined in addition to other criteria. Lipinski (Pfizer), Ghose (Amgen), Veber (GSK), Egan (Pharmacia), and Muegge (Bayer) [20] are different rules that are searched by drug companies for drug candidates. The ABTH compound synthesized within the scope of the study met all these rules, as shown in Table 2.

For the LD_{50} values, toxic dosage limits are often expressed as mg/kg body weight. The dosage at which 50% of test subjects pass away after being exposed to a substance is known as the median lethal dose, or LD50. The globally harmonized method of classifying and labeling substances (GHS) establishes toxicological classifications. The classes were arranged from worst to best, from non-toxic to deadly, and from first to sixth. Protox-II web server, a popular tool to calculate toxicity in chemical compounds, was used to determine the toxicity features of ABTH. When Table 2 was examined, LD_{50} (Lethal Dose) value of ABTH was found to be 1440 mg/kg. The toxicity class of ABTH was also determined by using Protox-II web server. It was found to be fourth class, when the toxicity level was from 1st (the worst) to 6th (the best).

Table 2. ADMEt properties of ABTH

Physicochemical Properties		Druglikeness Properties		
Properties	Value ABTH	Requirement	Value ABTH	Compatible ABTH
		Lipinski's Rule		
Molecular Formula	$C_{15}H_{12}F_3N_3O$	MW ≤ 500	307.27	Yes
Molecular weight (MW, g/mol)	307.27	M LOGP ≤ 4.15	3.17	
Number of heavy atoms	22	HBA Atoms ≤ 10	5	
Number of aromatic heavy atoms (AHA)	12	HBD Atoms ≤ 5	2	
Number of rotatable bonds (RB)	5	Ghose's Rule		
Number of H-bond acceptors (HBA)	5	160 ≤ MW ≤ 480	307.27	
Number of H-bond donors (HBD)	2	-0.4 ≤ WLOGP ≤ 5.6	4.21	
Molar Refractivity (MR)	77.02	40 ≤ MR ≤ 130	77.02	
TPSA (Å²)	67.48	20 ≤ atoms ≤ 70	34	
Lipophilicity		Veber's Rule		
Log $P_{o/w}$ (iLOGP)	2.16	RB ≤ 10	5	Yes
Log $P_{o/w}$ (XLOGP3)	3.59	TPSA ≤ 140	67.48	
Log $P_{o/w}$ (WLOGP)	4.21	Egan's Rule		
Log $P_{o/w}$ (MLOGP)	3.17	WLOGP ≤ 5.88	4.21	Yes
Consensus Log $P_{o/w}$	3.28	TPSA ≤ 131.6	67.48	
Pharmacokinetics		Muegge's Rule		
GI absorption	High	200 ≤ MW ≤ 600	307.27	Yes
BBB permeant	Yes	-2 ≤ XLOG3 ≤ 5	3.59	
P-gp substrate	No	TPSA ≤ 150	67.48	
CYP1A2 inhibitor	Yes	Number of rings ≤ 7	2	
CYP2C19 inhibitor	No	Number of carbon > 4	15	
CYP2C9 inhibitor	No	Number of heteroatoms > 1	4	
CYP2D6 inhibitor	No	RB ≤ 15	5	
CYP3A4 inhibitor	No	HBA ≤ 10	5	
Log K_p (skin permeation, cm/s)	-5.63	HBD ≤ 5	2	
Water Solubility		Toxicity Properties		
Log S (ESOL)	-4.08	LD_{50} (mg/kg)	1440	
Class	Moderately soluble			
Log S (Ali)	-4.69	Toxicity Class	4	
Class	Moderately soluble			
Log S (SILICOS-IT)	-5.52			
Class	Moderately soluble			

Figure 7. depicts the Boiled-Egg model, with TPSA on the x-axis and WLOGP on the y-axis. The model's yellow region determines whether or not the drug crosses the BBB, while the white region is in charge of gastrointestinal absorption. It was determined by looking at the Boiled-Egg model in Figure 6 that the red dot was in the yellow region and chemical ABTH passed to the BBB.

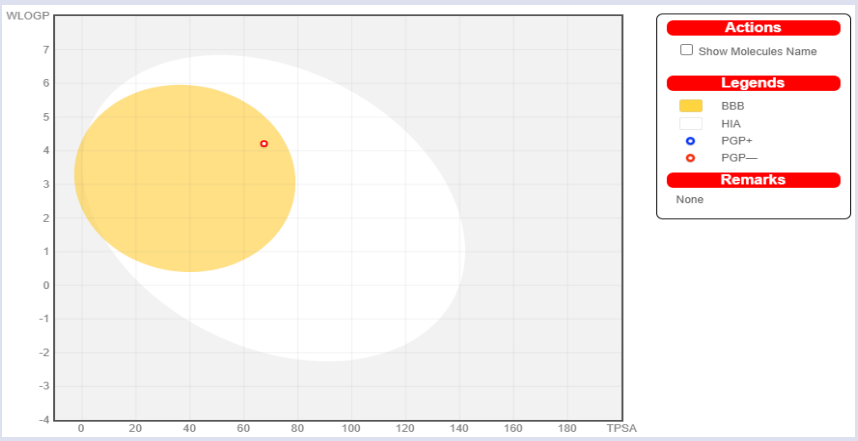

Figure 7. Boiled-Egg representation of ABTH

Molecular Docking Studies

Molecular docking studies was performed using AutoDock Vina 1.1.2 software. AD related proteins [34] were chosen for the molecular docking studies. The primary link between APP and Alzheimer's disease is its involvement in the synthesis of amyloid-beta (Aβ) peptides, which leads to the development of amyloid plaques. The typical symptoms of Alzheimer's disease, including memory loss and cognitive decline, are brought on by these plaques, which impair neuronal function, cause inflammation, and contribute to neurodegeneration. Developing therapies to stop or reduce Alzheimer's disease requires an understanding of APP processing and how it contributes to the illness's progression [35]. Understanding the structure of the ACE protein is essential to comprehending its enzymatic activity, which includes its function in the breakdown of Aβ. Through its impacts on vascular health and amyloid metabolism, ACE may have a doubled influence on Alzheimer's disease. The relationship is complicated, though, and further research is required to determine whether ACE or its inhibitors can be successfully targeted in Alzheimer's treatments [36]. BACE1 is an aspartic acid protease that plays a crucial role in the development of Alzheimer's disease by initiating the production of Aβ peptides. The primary function of the aspartic acid protease BACE1 is in Alzheimer's disease (AD). A crucial stage in the synthesis of Aβ peptides, it is in charge of the first cleavage of the amyloid precursor protein (APP) at the βsite. Alzheimer's disease is characterized by plaques that are formed in the brain by the accumulation of these peptides. The 4DJU structure is crucial in knowing how to block BACE1, an enzyme that is essential to the pathophysiology of Alzheimer's disease. This knowledge provides a basis for creating treatment approaches that target Alzheimer's disease [37, 38]. The 1Q5K structure provides crucial structural information for the creation of more powerful and selective medications by demonstrating precisely how AR-A014418 binds to GSK-3, which is crucial for the development of GSK-3 inhibitors. The development of focused treatments for Alzheimer's disease may benefit from this [39]. The activation of TNFα, a cytokine implicated in neuroinflammation linked to Alzheimer's disease, is significantly influenced by TACE. PDB entry 2OI0, which represents the crystal structure analysis, provides important information for the creation of specific TACE inhibitors, which may be used as therapeutic medicines to modulate neuroinflammation in Alzheimer's disease [40].

In view of given informations above, the specified proteins (PDB ID: 1AAP, 1O86, 4DJU, 1Q5K, 2OI0) were selected for the molecular docking studies. Obtained results of ABTH with the selected proteins were depicted in Table 3. The standard drugs used in treatment of AD were also docked with the same proteins to do meaningful comparison. While the lowest docking score was found to be -6.9 kcal/mol between 1AAP and ABTH complex, the highest one -8.9 kcal/mol between 2OI0 and ABTH. The all protein-ABTH complexes showed higher docking scores than all protein-standard drugs.

Table 3. Molecular Docking scores of ABTH and Standard drugs with the selected proteins

	Docking Scores (kcal/mol)			
PDB ID	ABTH	Donepezil*	Galantamine*	Rivastigmine*
1AAP	-6.9	-7.9	-6.8	-6.0
1O86	-8.5	-8.9	-8.1	-6.5
4DJU	-8.6	-6.9	-7.8	-6.6
1Q5K	-8.8	-8.4	-8.6	-6.5
2OI0	-8.9	-7.9	-7.3	-7.4

* Standard drugs

The 2OI0-ABTH complex, which has the highest score among all of protein-ligand complexes, were selected to investigate binding properties. The 2D figure, which contains binding properties bond types, and bond lengths, was demonstrated in Figure 8 and 3D figures in Table 4. When the 2D representation of 2OI0-ABTH complex was examined, it was observed that the complex has hydrogen bonds, hydrogen-carbon bonds, halogen, π-cation, π-donor hydrogen bond, π-π stacked, alkyl, and π-alkyl pairs. Among the protein-ligand interactions, hydrogen bonding is the most important one for the stability of the complex. When the 2D figure was examined, there were 3 hydrogen bonds 2OI0-ABTH complex. These bonds have a length of 2.51 Å between GLU406 aminoacid of protein and proton of amine group, 2.64 Å between HIS405 aminoacid and oxygen of carbonyl group, and 2.93 Å between HIS415 aminoacid and oxygen of carbonyl group. Halogen interactions were also observed in 2OI0-ABTH complex. These bonds were between ABTH and LEU401, VAL434 aminoacids with the 3.12, 3.39, 3.44 Å, respectively.

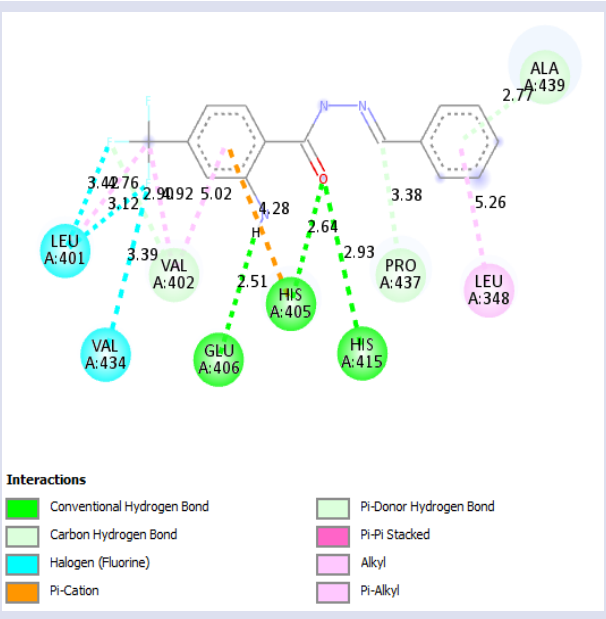

Figure 8. 2D representation of 2OI0-ABTH complex

Table 4. 3D interactions and hydrophobicity surfaces of 2OI0-ABTH complex

a) Zoom out interaction

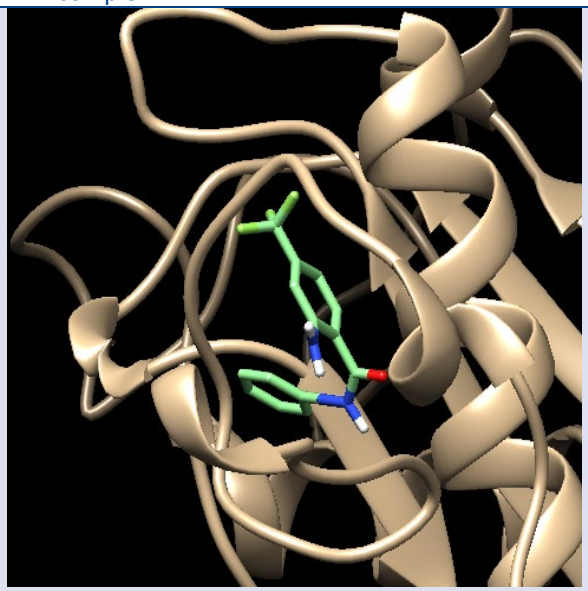

b) Zoom in interaction

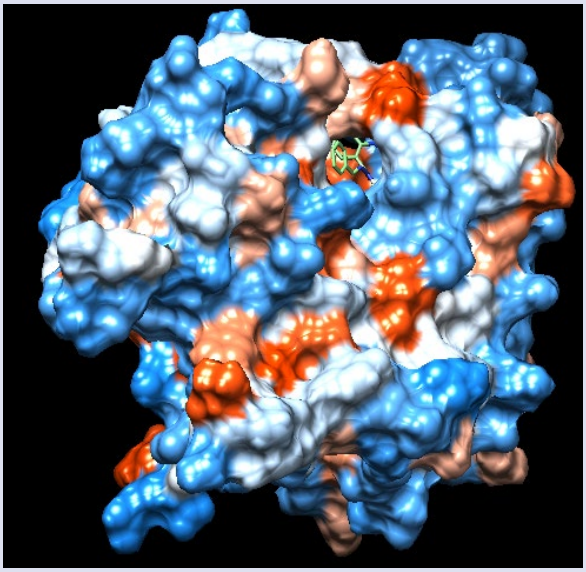

c) Zoom out hydrophobicity

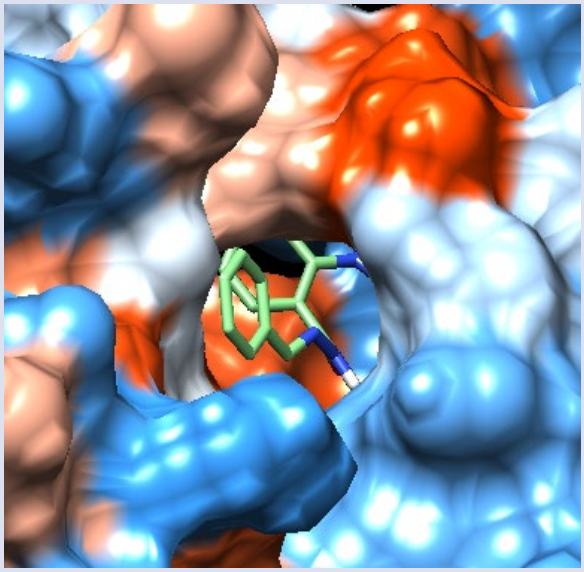

d) Zoom in hydrophobicity

MD Simulation Studies

Stability of the 2OI0-ABTH system was investigated utilizing MD simulation via playmolecule web server during 12 ns. For the MD simulation investigation, the RMSD (Root Mean Square Deviations) of the ligand and system's sidechain/backbone values were determined. The RMSD graph was depicted in Figure 9. For the backbone/sidechain value, the mean RMSD was 2.5 Å, whereas for the ABTH ligand, it was 1.5 Å. During the 12 ns MD simulation, the backbone/sidechain's RMSD graph remained unchanged. For the complex to be stable, the RMSD value needs to be less than 3 Å. The 2OI0-ABTH complex's stability was confirmed by the RMSD values that were acquired from the MD simulation.

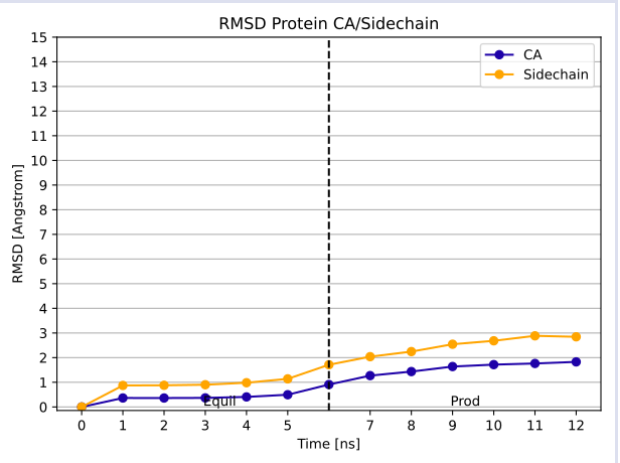

Figure 9. RMSD value of backbone and sidechain for the system during MD simulation

In molecular dynamics simulations, the term "RMSF" (Root Mean Square Fluctuation) describes how much individual atoms or groups of atoms move or fluctuate about their average position during the simulation. To calculate RMSF, the difference between each atom's average location and its positions at each time step is taken and its root mean squared. The stability or flexibility of different molecular constituents can be better understood by knowing how to analyze RMSF. Higher mobility or flexibility is correlated with lower RMSF values, which are correlated with greater stiffness or stability. RMSF values of 2OI0 were shown in Figure 10. Based on the calculated RMSF values, the residue index positions 150-160 had the biggest protein fluctuations during the simulation. In order to ensure the stability of the complex, the RMSF value must also be less than 3 Å. The 2OI0-ABTH complex's stability was further supported by the observation that, aside from these amino acids, the protein in the complex's structure changed very little. The complex's stability was also confirmed by the RMSF value, which was less than 3 (Figure 10).

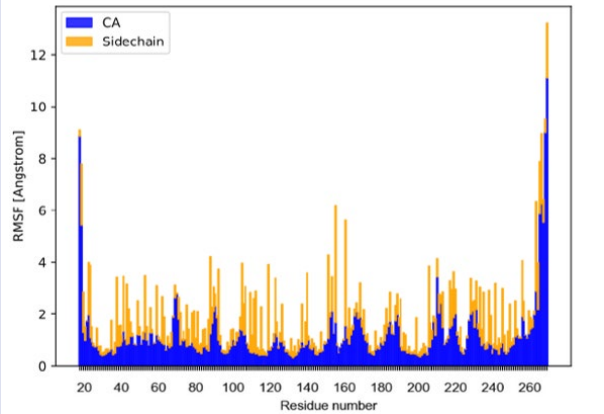

Figure 10. RMSF graph of protein (2OI0) during MD simulation

Conclusion

In this work, we synthesized a new compound as abbreviated ABTH, starting with carboxylic acid containing -CF_3 and -NO_2 groups. Its structure was characterized by spectroscopic methods such as NMR, FTIR, and Mass. ADMEt properties were investigated. From the results ABTH has all criteria in terms of druglikeness and crossed the BBB in terms of pharmacokinetic properties. Crossing the BBB is important to be potential drugs for treatment of AD. Target proteins associated with AD were chosen, and Molecular Docking studies were carried out by using these proteins. The highest docking score was -8.9 kcal/mol formed complex between 2OI0 protein and ABTH ligand. Standard drugs were also used in the molecular docking studies to compare whether ABTH has highest score or not. It was concluded that ABTH has higher docking score than standards. As the 2OI0-ABTH complex has the highest docking score, Additionally, a study using MD simulation was conducted to bolster the stability of the 2OI0-ABTH complex. The complex demonstrated to be stable during the 12 ns simulation, according to the MD simulation results. It can be concluded from all of the results that our synthesized ABTH is an effective candidate for AD, after deeply research have been performed.

Conflicts of interest

There are no conflicts of interest in this work.

Acknowledgment

The authors thanks to HUBTAM in Harran University for ^{1}H and ^{13}C-APT NMR analyses.

References

[1] Lu D., Sun Y., Luan Y., He W., Rational design of siRNA-based delivery systems for effective treatment of brain diseases, *Pharmaceutical Science Advances*, (2) (2024) 100041.

[2] Harder B.G., Blomquist M.R., Wang J., Kim A.J., Woodworth G.F., Winkles J.A., Loftus J.C., Tran N.L., Developments in Blood-Brain Barrier Penetrance and Drug Repurposing for Improved Treatment of Glioblastoma, *Frontiers in Oncology*, (8) (2018) 462.

[3] Burns A., Robert P., The National Dementia strategy in England, *BMJ*, (338) (2009) b931–b931.

[4] Brookmeyer R., Johnson E., Ziegler-Graham K., Arrighi H.M., Forecasting the global burden of Alzheimer's disease, *Alzheimer's & Dementia*, (3) (2007) 186–191.

[5] Hashimoto M., Rockenstein E., Crews L., Masliah E., Role of Protein Aggregation in Mitochondrial Dysfunction and Neurodegeneration in Alzheimer's and Parkinson's Diseases, *NeuroMolecular Medicine*, (4) (2003) 21–36.

[6] Hagmann W.K., The Many Roles for Fluorine in Medicinal Chemistry, *Journal of Medicinal Chemistry*, (51) (2008) 4359–4369.

[7] Nair A.S., Singh A.K., Kumar A., Kumar S., Sukumaran S., Koyiparambath V.P., Pappachen .LK., Rangarajan T.M., Kim H., Mathew B., FDA-Approved Trifluoromethyl Group-Containing Drugs: A Review of 20 Years, *Processes*, (10) (2022) 2054.

[8] Tatum L.A., Su X., Aprahamian I., Simple Hydrazone Building Blocks for Complicated Functional Materials, *Accounts of Chemical Research*, (47) (2014) 2141–2149.

[9] Verma G., Marella A., Shaquiquzzaman M., Akhtar M., Ali M., Alam M., A review exploring biological activities of hydrazones, *Journal of Pharmacy and Bioallied Sciences*, (6) (2014) 69.

[10] Rollas S., Küçükgüzel S., Biological Activities of Hydrazone Derivatives, *Molecules*, (12) (2007) 1910–1939.

[11] AlFadly E.D., Elzahhar P.A., Tramarin A., Elkazaz S., Shaltout H., Abu-Serie M.M., Janockova J., Soukup O., Ghareeb D.A., El-Yazbi A.F., Rafeh R.W., Bakkar N.M.Z., Kobeissy F., Iriepa I., Moraleda I., Saudi M.N.S., Bartolini M., Belal A.S.F., Tackling neuroinflammation and cholinergic deficit in Alzheimer's disease: Multi-target inhibitors of cholinesterases, cyclooxygenase-2 and 15-lipoxygenase, *European Journal of Medicinal Chemistry*, (167) (2019) 161–186.

[12] DiMasi J.A., Grabowski H.G., Hansen R.W., Innovation in the pharmaceutical industry: New estimates of R&D costs, *Journal of Health Economics*, (47) (2016) 20–33.
[13] Zhong F., Xing J., Li X., Liu X., Fu Z., Xiong Z., Lu D., Wu X., Zhao J., Tan X., Li F., Luo X., Li Z., Chen K., Zheng M., Jiang H., Artificial intelligence in drug design, *Science China Life Sciences*, (61) (2018) 1191–1204.
[14] Cui W., Aouidate A., Wang S., Yu Q., Li Y., Yuan S., Discovering Anti-Cancer Drugs via Computational Methods, *Frontiers in Pharmacology*, (11) (2020) 733.
[15] Ramírez D., Computational Methods Applied to Rational Drug Design, *The Open Medicinal Chemistry Journal*, (10) (2016) 7–20.
[16] De Vries H.E., Kuiper J., de Boer A.G., Van Berkel T.J., Breimer D.D., The blood-brain barrier in neuroinflammatory diseases. *Pharmacological Reviews*, (49) (1997) 143–155.
[17] Narayanan R., Gunturi S.B., In silico ADME modelling: prediction models for blood–brain barrier permeation using a systematic variable selection method, *Bioorganic & Medicinal Chemistry*, (13) (2005) 3017–3028.
[18] Karabacak Atay Ç., Dilek Ö., Tilki T., Dede B., A novel imidazole-based azo molecule: synthesis, characterization, quantum chemical calculations, molecular docking, molecular dynamics simulations and ADMET properties, *Journal of Molecular Modeling*, (29) (2023) 226.
[19] Karplus M., McCammon J.A., Molecular dynamics simulations of biomolecules, *Nature Structural & Molecular Biology*, (9) (2002) 646–652.
[20] Daina A., Michielin O., Zoete V., SwissADME: a free web tool to evaluate pharmacokinetics, drug-likeness and medicinal chemistry friendliness of small molecules, *Scientific Reports*, (7) (2017) 42717.
[21] Banerjee P., Eckert A.O., Schrey A.K., Preissner R., ProTox-II: a webserver for the prediction of toxicity of chemicals, *Nucleic Acids Research*, (46) (2018) W257–W263.
[22] Hanwell M.D., Curtis D.E., Lonie, Vandermeersch T., Zurek E., Hutchison G.R., Avogadro: an advanced semantic chemical editor, visualization, and analysis platform, *Journal of Cheminformatics*, (4) (2012) 17.
[23] Trott O., Olson A.J., AutoDock Vina: Improving the speed and accuracy of docking with a new scoring function, efficient optimization, and multithreading, *Journal of Computational Chemistry*, (31) (2010) 455–461.
[24] Pettersen E.F., Goddard T.D., Huang C.C., Couch G.S., Greenblatt D.M., Meng E.C., Ferrin T.E., UCSF Chimera--A visualization system for exploratory research and analysis, *Journal of Computational Chemistry*, (25) (2004) 1605–1612.
[25] BIOVIA, 2021 Discovery Studio Visualizer, version 21.1.0.20298. Dassault Systèmes, San Diego, CA.
[26] Berman H.M., The Protein Data Bank, *Nucleic Acids Research*, (28) (2000) 235–242.
[27] Webb B., Sali A., Comparative Protein Structure Modeling Using MODELLER, *Current Protocols in Bioinformatics*, (54) (2016) 5.6.1-5.6.37.
[28] Jiménez J., Doerr S., Martínez-Rosell G., Rose A.S., De Fabritiis G., DeepSite: protein-binding site predictor using 3D-convolutional neural networks, *Bioinformatics*, (33) (2017) 3036–3042.
[29] Martínez-Rosell G., Giorgino T., De Fabritiis G., PlayMolecule ProteinPrepare: A Web Application for Protein Preparation for Molecular Dynamics Simulations, *Journal of Chemical Information and Modeling*, (57) (2017) 1511–1516.
[30] Galvelis R., Doerr S., Damas J.M., Harvey M.J., De Fabritiis G., A Scalable Molecular Force Field Parameterization Method Based on Density Functional Theory and Quantum-Level Machine Learning, *Journal of Chemical Information and Modeling*, (59) (2019) 3485–3493.
[31] Doerr S., Harvey M.J., Noé F., De Fabritiis G., HTMD: High-Throughput Molecular Dynamics for Molecular Discovery, *Journal of Chemical Theory and Computation*, (12) (2016) 1845–1852.
[32] Veber D.F., Johnson S.R., Cheng H.Y., Smith B.R., Ward K.W., Kopple K.D., Molecular Properties That Influence the Oral Bioavailability of Drug Candidates, *Journal of Medicinal Chemistry*, (45) (2002) 2615–2623.
[33] Savjani K.T., Gajjar A.K., Savjani J.K., Drug Solubility: Importance and Enhancement Techniques, *International Scholarly Research Notices Pharmaceutics*, (2012) (2012) 1–10.
[34] Gnanaraj C., Sekar M., Fuloria S., Swain S.S., Gan S.H., Chidambaram K., Rani N.N.I.M., Balan T., Stephenie S., Lum P.T., Jeyabalan S., Begum M.Y., Chandramohan V., Thangavelu L., Subramaniyan V., Fuloria N.K, In Silico Molecular Docking Analysis of Karanjin against Alzheimer's and Parkinson's Diseases as a Potential Natural Lead Molecule for New Drug Design, Development and Therapy, *Molecules*, (27) (2022) 2834.
[35] Hardy J., Selkoe D.J., The Amyloid Hypothesis of Alzheimer's Disease: Progress and Problems on the Road to Therapeutics, *Science*, (297) (2002) 353–356.
[36] Qıu W., Folsteın M., Insulin, insulin-degrading enzyme and amyloid-β peptide in Alzheimer's disease: review and hypothesis, *Neurobiology of Aging,* (27) (2006) 190–198.
[37] Vassar R., Bennett B.D., Babu-Khan S., Kahn S., Mendiaz E.A., Denis P., Teplow D.B., Ross S., Amarante P., Loeloff R., Luo Y., Fisher S., Fuller J., Edenson S., Lile J., Jarosinski M.A., Biere A.L., Curran E., Burgess T., Louis J.-C., Collins F., Treanor J., Rogers G., Citron M., β-Secretase Cleavage of Alzheimer's Amyloid Precursor Protein by the Transmembrane Aspartic Protease BACE, *Science,* (286) (1999) 735–741.
[38] Ghosh A.K., Cárdenas E.L., Osswald H.L., The Design, Development, and Evaluation of BACE1 Inhibitors for the Treatment of Alzheimer's Disease, *Alzheimer's Disease II*, (2016) 27–85.
[39] Kremer A., GSK3 and Alzheimer's disease: facts and fiction…, *Frontiers in Molecular Neuroscience*, (4) (2011) 17.
[40] Plantone D., Pardini M., Righi D., Manco C., Colombo B.M., N. De Stefano, The Role of TNF-α in Alzheimer's Disease: A Narrative Review, *Cells,* 13 (2023) 54.